Dynamics around black holes: Radiation emission and Tidal effects

Richard Brito
Under supervision of Vitor Cardoso
CENTRA, Departamento de Física, Instituto Superior Técnico,
Universidade Técnica de Lisboa - UTL, Avenida Rovisco Pais 1, 1049 Lisboa, Portugal.
(Dated: November 5, 2012)

In this paper we study several dynamical processes involving black holes in four and higher dimensions. First, using perturbative techniques, we compute the massive scalar radiation emitted by a particle radially infalling into a Schwarzchild black hole. We show that the late-time waveform of massive scalar perturbations is dominated by a universal oscillatory decaying tail, which appears due to curvature effects. In the second part, we study the phenomenon of superradiance in higher dimensions and conjecture that the maximum energy extracted from a rotating black hole can be understood in terms of the ergoregion proper volume. We then study some consequences of superradiance in the dynamics of moons orbiting around higher-dimensional rotating black holes. In four-dimensional spacetime, moons around black holes generate low-amplitude tides, and the energy extracted from the hole's rotation is always smaller than the gravitational radiation lost to infinity. We show that in dimensions larger than five the energy extracted from the black hole through superradiance is larger than the energy carried out to infinity. Our results lend strong support to the conjecture that tidal acceleration is the rule, rather than the exception, in higher dimensions. Superradiance dominates the energy budget and moons "outspiral"; for some particular orbital frequency, the energy extracted at the horizon equals the energy emitted to infinity and "floating orbits" generically occur. We give an interpretation of this phenomenon in terms of tidal acceleration due to energy dissipation across the horizon.

Keywords: Black holes; Scalar fields; Extra dimensions; Superradiance; Tidal forces

I. INTRODUCTION

Black holes are the simplest macroscopic objects in the Universe. They are easily understood using only the concept of space and time given by General Relativity. Nowadays, it is universally recognized that black holes are not only of academic interest, but they are also of central importance in astrophysical processes and fundamental physics [1, 2].

Recently, the discovery of the gauge/gravity duality has given a whole new interest to the study of general spacetimes, and more particularly of black hole spacetimes. The most widely studied gauge/gravity duality is the AdS/CFT correspondence, which maps the dynamics of non-Abelian conformal field theories (CFTs) in D-dimensional spacetimes onto semiclassical gravity in asymptotically Anti-de Sitter (AdS) spacetimes, i.e. , spacetimes with a negative cosmological constant, in $D+1$ dimensions [3, 4]. This duality could provide tools to understand the behavior of strongly coupled systems, impossible to describe using perturbative methods, in terms of AdS black holes that interact semiclassically with fields.

In addition to the AdS/CFT duality, in the last decades, there has been a growing interest in physical phenomena in higher dimensional spacetimes, mainly motivated by higher dimensional solutions which naturally arise in the context of string theories and supergravities. In some scenarios, the extra dimensions arise naturally as an attempt to solve the hierarchy problem. In some extra-dimensional models, if the extra dimensions are highly warped and correspond to a very large volume, the Planck scale can be as low as $M_{dPl} \sim \mathcal{O}(1)$ TeV, eliminating the large difference between this scale and the electroweak scale. These are the so-called *TeV-gravity* scenarios [5–9]. At the Planck scale, in some conditions, gravity can become highly non-linear, and black hole formation is expected [10, 11]. The formation of these higher-dimensional black holes would carry a clear signature through the decay by Hawking radiation, emission of gravitational waves, and in some theories, other types of radiation, such as scalar radiation, which could be detected at the LHC.

Purely analytical computations are normally only possible at a linear level and, in most cases, it is impossible to obtain a full analytical solution. In fact, solving the Einstein's equations exactly, i.e. , with no approximations, is a formidable task which requires supercomputers and sophisticated numerical methods. Complementary to these, semianalytical methods are instrumental for a better understanding of dynamical processes in General Relativity and sometimes for interpreting the results of the simulations. On the other hand, even using a perturbative approach usually requires numerical solutions. The development of these complementary approaches cannot be done independently. This is the main motivation of this work, to study and understand processes that could be seen in future numerical simulations and could also be of great importance, both in the astrophysical context and in more theoretical applications, like the gauge/gravity duality and TeV-gravity scenarios.

This work is organized as follows. In section II we compute the fundamental equations of scalar radiation in terms of black hole perturbations sourced by a test-

particle in geodesic motion around a spinning black hole. We derive the Teukolsky equations and solve the wave equation using the Green's functions approach. In section III we specialize the problem to the case of a particle falling radially into a Schwarzschild black hole. We compute the massive scalar radiation waveforms emited by the particle and the correspondent energy spectra. In section IV we study the superradiant scattering of a massless scalar field with a singly spinning black hole in $D = 4 + n$ dimensions. In section V we compute the energy fluxes in terms of black hole perturbation theory sourced by a test-particle in circular orbit around a spinning black hole, both analytically and numerically. We conclude in section VI. Throughout the paper we use $G = c = \hbar = 1$ units.

II. SCALAR PERTURBATIONS OF SINGLY SPINNING MYERS–PERRY BLACK HOLES

The way a black hole reacts to external perturbations provides us with a deep understanding of the space-time around it. Here we will be interested, more particularly, in scalar perturbations of singly-spinning Myers–Perry black holes due to the presence of a test particle coupled to the scalar field. The results here derived will serve as a framework for the subsequent sections.

A. The background metric

In four dimensions, there is only one possible angular momentum parameter for an axisymmetric spacetime, and rotating black hole solutions are uniquely described by the Kerr family. In higher dimensions there are several choices of rotation axis, which correspond to a multitude of angular momentum parameters [12]. Here we shall focus on the simplest case, where there is only a single axis of rotation. In the following we shall adopt the notation used in Refs. [13–15], to which we refer for details.

The metric of a $(4+n)$-dimensional Kerr–Myers–Perry black hole with only one nonzero angular momentum parameter is given in Boyer–Lindquist coordinates by [12]

$$\begin{aligned} ds^2 = &-\frac{\Delta - a^2\sin^2\vartheta}{\Sigma}dt^2 - \frac{2a(r^2+a^2-\Delta)\sin^2\vartheta}{\Sigma}dtd\phi \\ &+ \frac{(r^2+a^2)^2 - \Delta a^2\sin^2\vartheta}{\Sigma}\sin^2\vartheta d\phi^2 + \frac{\Sigma}{\Delta}dr^2 \\ &+ \Sigma d\vartheta^2 + r^2\cos^2\vartheta d\Omega_n^2\,, \end{aligned} \tag{1}$$

where

$$\Sigma = r^2 + a^2\cos^2\vartheta\,, \qquad \Delta = r^2 + a^2 - 2Mr^{1-n}\,, \tag{2}$$

and $d\Omega_n^2$ denotes the standard line element of the unit n-sphere.

The event horizon is located at $r = r_H$, defined as the largest real root of Δ. In four dimensions, an event horizon exists only for $a \leq M$. In five dimensions, an event horizon exists only for $a \leq \sqrt{2M}$, and the black hole area shrinks to zero in the extremal limit $a \to \sqrt{2M}$. On the other hand, when $D > 5$, there is no upper bound on the black hole spin and a horizon exists for any a.

B. The wave equation

We consider a small object in a geodesical curve around a spinning black hole and a scalar field of mass $m_s = \mu\hbar$ coupled to matter (from now on we set $\hbar = 1$. In these units μ has the dimensions of 1/length). At first order in perturbation theory, the scalar field equation in the background (1) reads

$$\Box\varphi - \mu^2\varphi \equiv \frac{1}{\sqrt{-g}}\frac{\partial}{\partial x^\mu}\left(\sqrt{-g}g^{\mu\nu}\frac{\partial}{\partial x^\nu}\varphi\right) - \mu^2\varphi = \alpha\mathcal{T}\,, \tag{3}$$

where α is some coupling constant. For simplicity we focus on source terms of the form

$$\mathcal{T} = -\int \frac{d\tau}{\sqrt{-g}}q_p\delta^{(4+n)}(x - X(\tau))\,, \tag{4}$$

which corresponds to the trace of the stress-energy tensor of a point particle with scalar charge q_p.

Because of the coupling to matter, the object emits scalar radiation, which is governed by Eq. (3). To separate Eq. (3), we consider the ansatz

$$\varphi(t, r, \vartheta, \phi) = \sum_{l,m,j}\int d\omega e^{im\phi - i\omega t}R(r)S_{lmj}(\vartheta)Y_j\,, \tag{5}$$

where Y_j are hyperspherical harmonics [14, 16] on the n-sphere with eigenvalues given by $-j(j+n-1)$ and j being a non-negative integer. The radial and angular equations read

$$\begin{aligned} r^{-n}\frac{d}{dr}\left(r^n\Delta\frac{dR}{dr}\right) + \Bigg\{&\frac{\left[\omega(r^2+a^2) - ma\right]^2}{\Delta} \\ &- \frac{j(j+n-1)a^2}{r^2} - \lambda\Bigg\}R = T_{lmj}\,, \end{aligned} \tag{6}$$

and

$$\begin{aligned} \frac{1}{\sin\vartheta\cos^n\vartheta}\frac{d}{d\vartheta}\left(\sin\vartheta\cos^n\vartheta\frac{dS_{lmj}}{d\vartheta}\right) + \Big[&\omega^2a^2\cos^2\vartheta \\ &- \frac{m^2}{\sin^2\vartheta} - \frac{j(j+n-1)}{\cos^2\vartheta} + A_{lmj}\Big]S_{lmj} = 0\,, \end{aligned} \tag{7}$$

where $\lambda = A_{lmj} - 2m\omega a + \omega^2a^2$, A_{lmj} are the eigenvalues of the angular equation, and we have defined

$$\alpha\Sigma\mathcal{T} = \sum_{l,m,j}\int d\omega e^{im\phi - i\omega t}T_{lmj}S_{lmj}(\vartheta)Y_j\,. \tag{8}$$

Defining a new radial function $X_{lmj}(r)$

$$X_{lmj} = r^{n/2}(r^2+a^2)^{1/2}R\,, \tag{9}$$

we get the nonhomogeneous equation for the scalar field

$$\left[\frac{d^2}{dr_*^2}+V\right]X_{lmj}(r^*)=\frac{\Delta}{(r^2+a^2)^{3/2}}r^{n/2}T_{lmj}\,, \quad (10)$$

where $dr/dr_*=\Delta/(r^2+a^2)$ defines the standard tortoise coordinates and the effective potential V is the one derived in Ref. [17].

In the low-frequency limit the angular Eq. (7) can be solved exactly. For the massless case $\mu=0$ and at first order in $a\omega$, the eigenvalues can be computed analytically [16]

$$A_{kjm}=(2k+j+|m|)(2k+j+|m|+n+1)+\mathcal{O}(a\omega)\,. \quad (11)$$

By setting $2k=l-(j+|m|)$, the eigenvalues above take the form $A_{ljm}=l(l+n+1)$ and l is such that $l\geq(j+|m|)$, which generalizes the four-dimensional case. An important difference from the four-dimensional case is that regularity of the angular eigenfunctions requires k to be a non-negative integer; i.e. for given j and m only specific values of l are admissible. In fact, it is convenient to label the eigenfunctions and the eigenvalues with the "quantum numbers" (k,j,m) rather than with (l,j,m) as in the four-dimensional case.

The (non-normalized) zeroth-order eigenfunctions are given in terms of hypergeometric functions [14, 16]

$$S_{kjm}\propto\sin(\vartheta)^{|m|}x^j F\Big[-k,k+j+|m|+\frac{n+1}{2},j+\frac{n+1}{2};x^2\Big]\,, \quad (12)$$

where $x=\cos(\vartheta)$. We adopt the following normalization condition:

$$\int_0^{\pi/2}d\vartheta\sin\vartheta\cos^n\vartheta S_{kjm}S^*_{kjm}=1\,, \quad (13)$$

where the integration domain has been chosen in order to have a nonvanishing measure also in the case of odd dimensions. Note that this normalization differs from that adopted in Ref. [16].

C. Green function approach

To solve the wave equation, let us choose two independent solutions $X^{r_H}_{kjm}$ and X^{∞}_{kjm} of the homogeneous equation, which satisfy the following boundary conditions:

$$\begin{cases} X^{\infty}_{kjm}\sim e^{ik_\infty r_*}\,, \\ X^{r_H}_{kjm}\sim A_{\rm out}e^{ik_\infty r_*}+A_{\rm in}e^{-ik_\infty r_*}\,, \end{cases} \qquad r\to\infty \quad (14)$$

$$\begin{cases} X^{\infty}_{kjm}\sim B_{\rm out}e^{ik_H r_*}+B_{\rm in}e^{-ik_H r_*}\,, \\ X^{r_H}_{kjm}\sim e^{-ik_H r_*}\,, \end{cases} \qquad r\to r_H\,. \quad (15)$$

Here $k_H=\omega-m\Omega_H, k_\infty=\sqrt{\omega^2-\mu^2}$, and $\Omega_H\equiv-\lim_{r\to r_H}g_{t\phi}/g_{\phi\phi}=a/(r_H^2+a^2)$ is the angular velocity at the horizon of locally nonrotating observers. The Wronskian of the two linearly independent solutions reads

$$W=X^{r_H}_{kjm}\frac{dX^{\infty}_{kjm}}{dr_*}-X^{\infty}_{kjm}\frac{dX^{r_H}_{kjm}}{dr_*}=2ik_\infty A_{\rm in}\,, \quad (16)$$

and it is constant by virtue of the field equations.

Imposing the usual boundary conditions, i.e. , only ingoing waves at the horizon and outgoing waves at infinity, Eq. (10) can be solved in terms of the Green function [18]

$$X_{kjm}(r_*)=\frac{X^{\infty}_{kjm}}{W}\int_{-\infty}^{r_*}T_{kjm}(r')\frac{\Delta r'^{n/2}}{(r'^2+a^2)^{3/2}}X^{r_H}_{kjm}dr'_* + \frac{X^{r_H}_{kjm}}{W}\int_{r_*}^{\infty}T_{kjm}(r')\frac{\Delta r'^{n/2}}{(r'^2+a^2)^{3/2}}X^{\infty}_{kjm}dr'_*\,. \quad (17)$$

III. SCALAR RADIATION FROM AN INFALL OF A PARTICLE INTO A SCHWARZSCHILD BLACK HOLE

Let us specialize the results derived in the last section to the case of a particle radially infalling into a Schwarzschild black hole coupled to a massive scalar field.

A. Basic Fomalism

We consider a test particle with scalar charge q_p and gravitational mass m_p, and a massive scalar field coupled to matter, falling into a Schwarzschild black hole along a radial timelike geodesic.

Using the framework introduced in section II we arrive at a wavefunction for the scalar field whose evolution is given by the wave equation

$$\left[\frac{d^2}{dr_*^2}+(\omega^2-V(r))\right]\tilde{X}(\omega,r)=f(r)S\,, \quad (18)$$

where the potential V is given by,

$$V=f(r)\left(\mu^2+\frac{l(l+1)}{r^2}+\frac{2M}{r^3}\right)\,. \quad (19)$$

Note that this equation corresponds to the wave equation (10), setting $a=0$, $n=0$ and redefining the source term in a way that it coincides with the literature [19]. The source term S depends uniquely on the stress-energy tensor and on the geodesic the particle follows. For massive particles, the radial timelike geodesics can be written as,

$$\frac{dT}{dr}=-\frac{E}{f(r)\sqrt{E^2-1+2M/r}}\,, \quad \frac{dT}{d\tau}=-\frac{E}{f(r)}\,, \quad (20)$$

where E is a conserved energy parameter. If we consider a particle with velocity v_∞ at infinity, then, $E=\frac{1}{(1-v_\infty^2)^{1/2}}\equiv\gamma$.

For a massive point particle the source S is given by,

$$S = -\frac{q_p}{\sqrt{2\pi r}} Y^*_{lm}(0,0) e^{i\omega T(r)} (\frac{dr}{d\tau})^{-1} . \quad (21)$$

Here, $Y_{lm}(\theta,\phi)$ are the spherical harmonics and the particle velocity is given by $\frac{dr}{d\tau} = -\sqrt{E^2 - 1 + 2M/r}$.

The energy spectra is given by

$$\frac{dE}{d\omega} = \omega\sqrt{\omega^2 - \mu^2}|\tilde{X}(\omega, r)|^2 , \quad (22)$$

and to reconstruct the wavefunction as a function of the time t we use the inverse Fourier transform

$$X(t,r) = \frac{1}{\sqrt{2\pi}} \int_{-\infty}^{+\infty} e^{-i\omega t} \tilde{X}(\omega, r) d\omega . \quad (23)$$

To find $\tilde{X}(\omega, r)$ we use the Green's function technique described in chapter II. Using Eq. (17) we get, at infinity,

$$\tilde{X}(\omega, r \to \infty) = \frac{e^{i\sqrt{\omega^2-\mu^2}\, r_*}}{W} \int_{r_H}^{\infty} X^{r_H} \, S \, dr . \quad (24)$$

B. Numerical Results

The energy spectra for the massive scalar field ($\mu M = 0.05$) is shown in Fig. 1. The field mass acts as lower cutoff since no energy can be radiated for frequencies below the field mass. We can also see that the quasinormal frequency of the black hole acts as a upper cutoff.

The waveforms for a scalar field of mass $\mu M = 0.05$ at a fixed radius $r_* = 10M$, are given in Fig. 2. For the quadrupolar mode $l = 2$, at late times, the signal is clearly dominated by the quasinormal ringing with frequency $\omega \sim 0.48/M$. However in the lowest radiatable modes, $l = 0$ and $l = 1$, the quasinormal ringing does not seem to appear even at intermediate late times. Instead the signal is dominated by a tail of the form $X \sim t^{-5/6}\sin(\mu t)$, independent of the angular number l. This is shown in Fig. 3 where we can see that this tail fits very well the numerical curve at late times. The contribution from the l dependent tail already present in the Minkowsky spacetime [20, 21] $X \sim t^{-(l+3/2)}\sin(\mu t)$ is also shown, and it is clear that at intermediate late-times this contribution is not negligible.

It is important to point that the curvature dependent tail $X \sim t^{-5/6}\sin(\mu t)$ is quite universal not only because it does not depend on l, but also because it appears also in Kerr black holes [22], and for other massive fields (Dirac [22, 23] and Proca [24]). It is thus expected that this behavior is universal for massive fields and does not depend on the details of the black hole horizon geometry [24]. Therefore, the signal emitted by the lowest multipoles of the massive scalar radiation does not give us much information about the black hole parameters, but can give us information about the field mass. This behavior was also found for other values of the mass μ, thus confirming our results.

IV. SUPERRADIANCE IN $4+n$ DIMENSIONS

Consider a Kerr black hole whose angular velocity of the horizon is Ω_H. A wave with frequency $\omega < m\Omega_H$ scattering off the black hole (where m is the azimuthal quantum number) is amplified, and it extracts rotational energy from the black hole. This phenomenon is known for many years under the name of *superradiance* [25–28]. We will see in the next section that superradiance is responsible for strong tidal effects around higher-dimensional rotating black holes. Therefore, in the context of this work, studying the phenomenon of superradiance in higher-dimensional rotating black holes is an interesting topic. In this section we shall use the framework introduced in section II to compute the energy amplification of a massless scalar field scattering off a singly spinning Myers–Perry black hole due to superradiance.

A. Numerical Results

In Fig. 4 we show the maximum amplification as a function of the spin parameter in different dimensions. To evaluate $A_{\max}$ for a given a, we varied the frequency in order to find a maximum for the amplification, and then repeated this for each value of a. The higher the dimension, the less the wave is amplified. In $D = 4$ (upper-left panel), the amplification increases with the rotation of the black hole and approaches the maximum value, $A_{\max} \sim 0.366\%$, at $a = 0.99M$. In $D = 5$ (upper-right panel)the amplification doesn't always grow as it would be naively expected. In fact, it grows until $a \sim 1.2M^{1/2}$, and then decreases until the extremal limit $a = (2M)^{1/2}$. This behavior is also seen in higher dimensions. In $D = 6$ and $D = 7$ (lower panels), where there is no upper bound on the black hole spin, the amplification factor doesn't increase without limit as we go to large spins. Instead, for large spins the superradiant amplification decreases and eventually becomes negligible.

The behavior of the maximum amplification factor with the black hole spin, can be partially understood computing the proper volume of the ergoregion as a function of the black hole spin. The proper volume can be computed using [29],

$$V = 4\pi \int_0^{2\pi} d\theta_n \int_0^{\pi} \prod_{i=1}^{n-1} d\theta_i \int_0^{\pi/2} d\vartheta \int_{r_i}^{r_f} dr \sqrt{g_{rr} g_{\vartheta\vartheta} g_{\phi\phi} \prod_{i=1}^{n} g_{\theta_i\theta_i}} , \quad (25)$$

In Fig. 5 we show the proper volume of the ergoregion as a function of the spin parameter in different dimensions. In $D = 4$ (upper-left panel) the proper volume grows monotonically with a/M, diverging for $a = M$. On the other hand, in higher dimensions, the proper volume increases with the black hole spin, for small spins, but

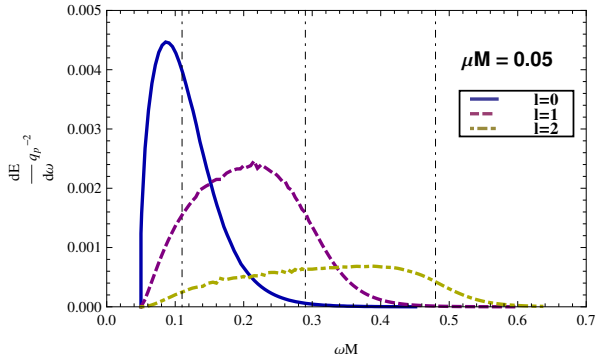

FIG. 1. Energy spectra of the massive scalar field of mass $\mu M = 0.05$ for the three lowest multipoles, for a massive particle falling from infinity into a Schwarzschild black hole with $E = 1.5$. The vertical lines correspond to the real part of the fundamental quasinormal mode for $l = 0$, $l = 1$ and $l = 2$ given respectively by, $M\omega_R = 0.11$, $M\omega_R = 0.29$, and $M\omega_R = 0.48$.

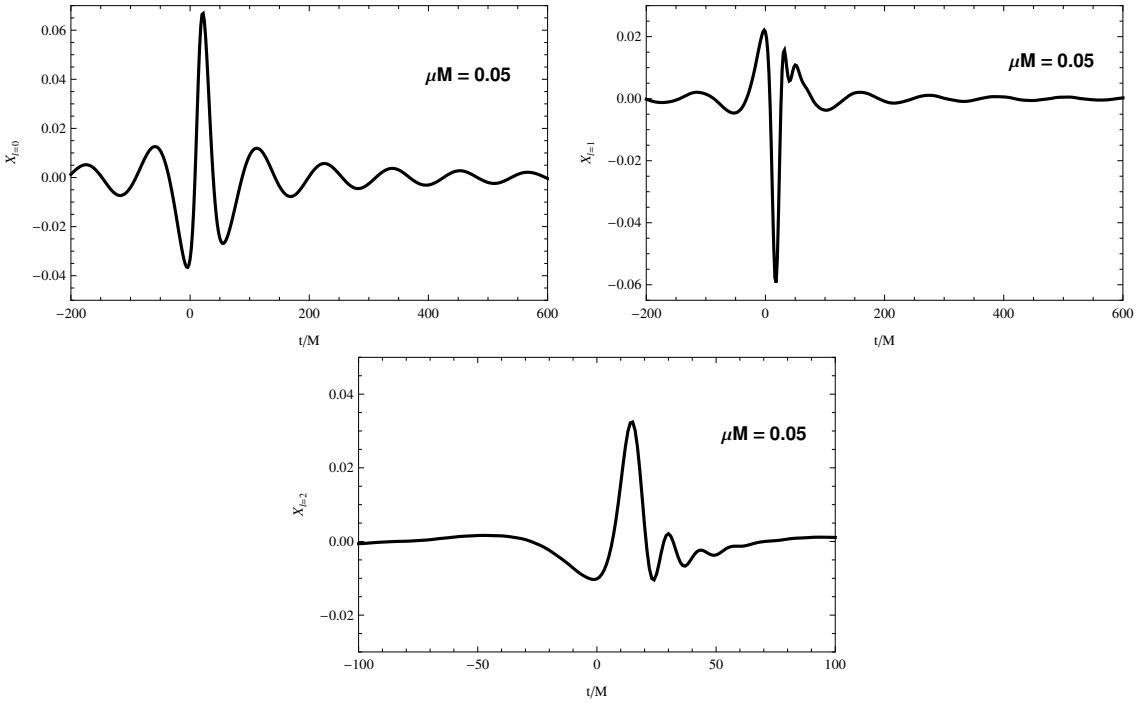

FIG. 2. Waveforms of the massive scalar radiation of mass $\mu M = 0.05$ for the three lowest multipoles at $r_* = 10M$, for a massive particle falling from infinity into a Schwarzschild black hole with $E = 1.5$. Here, the wavefunction X is measured in units of q_p.

eventually reaches a maximum value and then decreases monotonically with $a/M^{1/(1+n)}$.

Comparing Fig. 4 and Fig. 5, it is evident that there exist a correlation between the proper volume of the ergoregion and the superradiant amplification. This explains why the maximum amplification factor does not grow without limit as we increase the spin. At high spins the ergoregion proper volume goes to zero, constraining the energy extracted from the black hole. In fact, energy extraction from the black hole via superradiance is related to the existence of an ergoregion. Inside the ergoregion negative energy states are possible. If one scatter a wave off the black hole, the wave can excite negative energy modes which will fall into the black hole and extract energy from it. If the proper volume of the ergoregion goes to zero, then the wave will spend less time inside the ergoregion, extracting less energy from the black hole and consequently, the maximum amplification factor will also asymptotically vanish.

An evident functional correlation between the maximum amplification and the ergoregion proper volume is difficult to find, and as we can see comparing Fig. 4 and

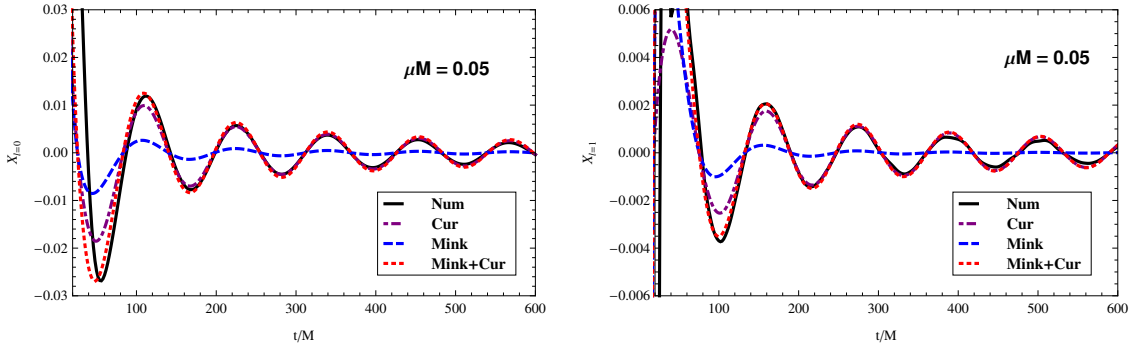

FIG. 3. Late-time tails of the massive scalar radiation ($\mu M = 0.05$) for the two lowest multipoles. The blue line corresponds to the theoretical contribution of the Minkowsky tail $X \sim t^{-(l+3/2)} \sin(\mu t)$, the purple line is the contribution of the curvature tail $X \sim t^{-5/6} \sin(\mu t)$ and the red line is the sum of the two tails.

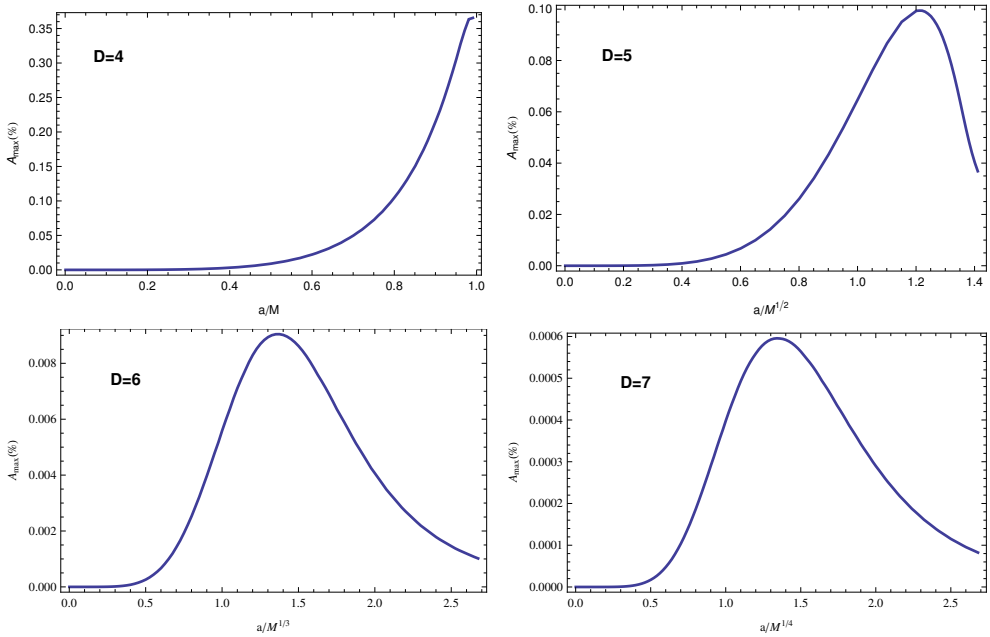

FIG. 4. Maximum amplification factor $A_{\max}$ as a function of the spin parameter a for the $l = m = 1, j = 0$ mode. Top: when D=4 (left), the maximum amplification grows with the spin parameter and approaches $A_{\max} \sim 0.366\%$ at $a = 0.99M$. When D=5 (right) the maximum amplification grows with the spin parameter until $a \sim 1.2M^{1/2}$ and then decreases monotonically. Bottom: in $D = 6$ (left), and $D = 7$ (right) the maximum amplification factor increases monotonically until $a \sim 1.4M^{1/(n+1)}$ and then decreases for large spins.

Fig. 5, the maximum peak of the amplification factor and of the proper volume does not occur at the same value of the spin a. However, it is interesting to note that, for $a > 1.5M^{1/(1+n)}$, $A_{\max}$ grows linearly with the ergoregion proper volume. Fitting the data to

$$A_{\max} = a_1 + b_1 V\,, \tag{26}$$

we find, for $D = 6$,

$$a_1 = 0.000500012\,, \quad b_1 = 0.000345673\,, \tag{27}$$

and, for $D = 7$,

$$a_1 = -0.000074633\,, \quad b_1 = 0.000034944\,. \tag{28}$$

We checked this linear relation between the maximum amplification and the ergoregion proper for large spins up to $D = 9$, which led us to say that it should be valid for any dimension.

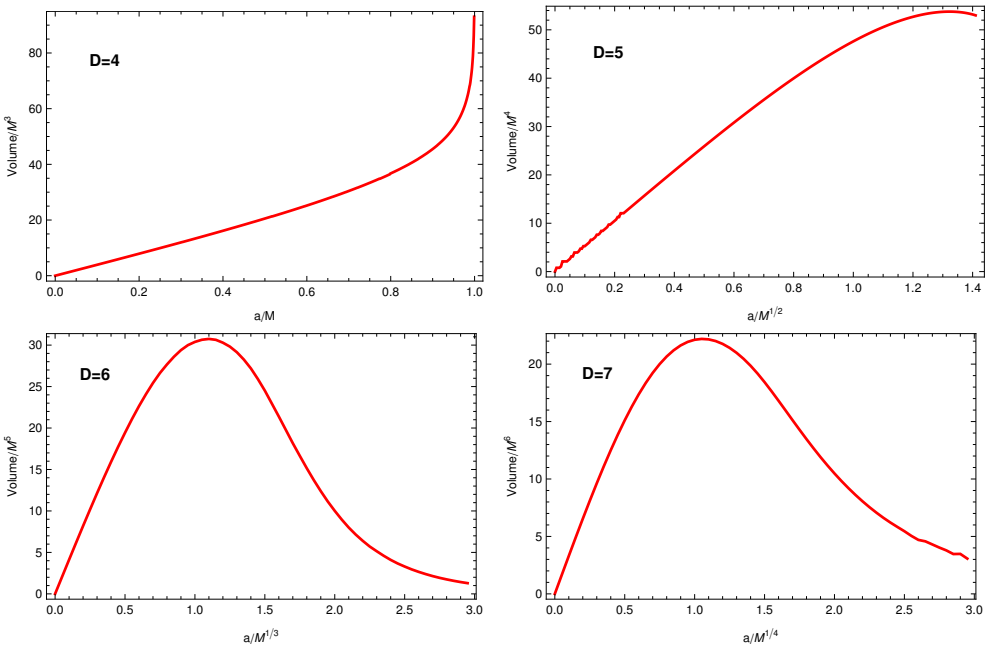

FIG. 5. Proper volume of the ergoregion as a function of the spin parameter $a/M^{1/(1+n)}$.

V. TIDES FOR CHARGED INTERACTIONS IN $4+n$ DIMENSIONS

It was recently argued via a tidal analysis framework that higher-dimensional black holes in general relativity should be prone to strong tidal effects [28]. One of the consequences of those studies was that orbiting bodies around higher-dimensional rotating black holes always spiral *outward*, if the tidal acceleration (or, equivalently, the superradiance) condition is met. In this section, we use a fully relativistic analysis, albeit in the test-particle limit, to prove this behavior.

A. Tidal acceleration: Analytical solution at low frequencies

Here we solve the wave equation, Eq. (10), analytically in the low-frequency regime (see e.g. [30–34]), obtaining a formula for the scalar flux which will be compared with the results obtained by a direct numerical integration of the wave equation.

1. Setup

We will restrict to equatorial circular orbits ($\dot{\vartheta}=0$, $\vartheta=\pi/2$), which is an unrealistic approximation in higher dimensions: generic circular orbits are unstable, with an instability time scale of order of the orbital period [35]. Nevertheless, our purpose here is to show that tidal effects can dominate, and it is not clear what the overall combined effect of tidal acceleration and circular geodesic motion instability is.

The source term T_{kmj} is given, in this case, by

$$T_{kmj} = -\frac{q_p \alpha}{U^t r^n} S^*_{kmj}(\pi/2) Y^*_j(\pi/2,\pi/2,\ldots) \times \delta(r-r_0)\delta(m\Omega_p-\omega)\,, \tag{29}$$

We note that at $\vartheta=\pi/2$ only higher dimensional spheroidal harmonics with $j=0$ are nonvanishing. This can be seen from Eq. (12). Thus, in order to calculate the fluxes on circular orbits, one only needs to consider terms with $j=0$. In this case, the hyperspherical harmonics Y_0 are constant.

Using the Green's function approach we can derive formulae for the energy fluxes at infinity and at the horizon.

The scalar energy flux at the horizon and at infinity are defined are given by [17]

$$\dot{E}_{H,\infty} = \sum_{kjm} m\Omega_p k_{H,\infty} |Z^{r_H,\infty}_{kjm}|^2\,, \tag{30}$$

where

$$Z^{r_H,\infty}_{kjm} = -\alpha \frac{X^{\infty,r_H}_{kjm}(r_0)}{WU^t} \frac{S^*_{kjm}(\pi/2) Y^*_j(\pi/2,\pi/2,\ldots)}{\sqrt{r_0^2+a^2} r_0^{n/2}} q_p\,, \tag{31}$$

which has been derived using Eq. (17) and Eq. (29). The equation above shows that, if the superradiant condition $k_H<0$ ($\omega<m\Omega_H$) is met, the energy flux at the horizon can be *negative*; $\dot{E}_H<0$, i.e. energy can be extracted from a spinning black hole [27, 36]. In four dimensions, $|\dot{E}_H| \ll \dot{E}_\infty$ and the superradiant extraction is generically negligible. As we show below, in higher dimensions

the opposite is true, $|\dot{E}_H| \gg \dot{E}_\infty$ and superradiance dominates over gravitational-wave emission.

2. Solution $X^{r_H}_{kjm}$

Let us first focus on the solution $X^{r_H}_{kjm}$, which is regular at the horizon. The derivation of the solution can be seen in [17], here we will only outline the principal results.

We first make the following change of variable:

$$h = \frac{\Delta}{r^2+a^2} \Rightarrow \frac{dh}{dr} = (1-h) r \frac{A(r)}{r^2+a^2}\,, \tag{32}$$

where $A(r) = (n+1) + (n-1)a^2/r^2$. Then, near the horizon $r \sim r_H$, the radial Eq. (6) can be written as

$$h(1-h)\frac{d^2R}{dh^2} + (1-D_* h)\frac{dR}{dh} + \left[\frac{P^2}{A(r_H)^2 h(1-h)} - \frac{\Lambda}{r_H^2 A(r_H)^2 (1-h)}\right] R = 0\,, \tag{33}$$

where

$$P = \omega(r_H + a^2/r_H) - ma/r_H\,, \tag{34}$$

$$\Lambda = [l(l+n+1) + j(j+n-1)a^2/r_H^2](r_H^2+a^2)\,, \tag{35}$$

$$D_* = 1 - \frac{4a^2 r_H^2}{\left[(n+1)r_H^2 + (n-1)a^2\right]^2}\,. \tag{36}$$

The solution of Eq. (33) in the low-frequency regime, for small values of a/r_H, and in the region where $1-h \ll 1$ and $r \gg r_H$, can be shown to be given by

$$R \sim \frac{X^{r_H}_{kjm}}{r^{1+n/2}} \sim \frac{r^l}{(2M)^{\frac{2l+n+1}{2(n+1)}} r_H^{\frac{1}{2}}} \frac{\Gamma[1+2\alpha]\Gamma[2-D_*-2\beta]}{\Gamma[2-D_*+\alpha-\beta]\Gamma[1+\alpha-\beta]}\,. \tag{37}$$

It is useful to rewrite the radial Eq. (10) in terms of the dimensionless variable $z = \omega r$. At large distances and in the low-frequency limit Eq. (10) reads

$$\left[\frac{d^2}{dz^2} + 1 - \frac{J(J+1)}{z^2}\right] X_{kjm}(z) = 0\,. \tag{38}$$

where we used the fact that at large distances the eigenvalues take the form $A_{ljm} = l(l+n+1)$, and defined the non-negative quantum number $J(J+1) = l(l+n+1) + \frac{n}{2}(1+\frac{n}{2})$. The solution of this equation can be shown to have the asymptotic expansion

$$X^{r_H}_{kjm}(z \ll 1) \sim \frac{B z^{J+1}}{2^{J+1/2}\Gamma[J+3/2]}\left[1 + O(z^2)\right]\,. \tag{39}$$

Matching (39) to (37) we get

$$B = \frac{2^{J+1/2}\Gamma[J+3/2]\Gamma[1+2\alpha]\Gamma[2-D_*-2\beta]}{\Gamma[2-D_*+\alpha-\beta]\Gamma[1+\alpha-\beta]} \times \frac{(2M)^{1/(2n+2)}}{\epsilon^{(J+1)/(n+1)} r_H^{1/2}}\left[1 + O(\epsilon)\right]\,. \tag{40}$$

The parameter $A_{\rm in}$ can be extracted from the behavior of the solution of the equation (38) near $z = \infty$. Therefore, it is given by

$$A_{\rm in} = \frac{2^J \Gamma[J+3/2]\Gamma[1+2\alpha]\Gamma[2-D_*-2\beta]}{\sqrt{\pi}\Gamma[2-D_*+\alpha-\beta]\Gamma[1+\alpha-\beta]} \times \left(\frac{i}{\epsilon^{1/(n+1)}}\right)^{J+1} \frac{(2M)^{1/(2n+2)}}{r_H^{1/2}}\left[1 + O(\epsilon)\right]\,. \tag{41}$$

With all of this at hand, we can now compute the flux at infinity in the low-frequency regime. From Eqs. (30) and (31) we get

$$\dot{E}_\infty = m^2\Omega_p^2 \left|Z^\infty_{kjm}\right|^2 = = m^{2+2l+n}\left[\frac{\alpha q_p \sqrt{\pi}}{2^{l+n/2+1}\Gamma[l+n/2+3/2]}\right]^2 \times [(n+1)M]^{l+n/2+1} |S_{kjm}(\pi/2)|^2 |Y_j(\pi/2,\pi/2,\ldots)|^2 \times r_0^{-\frac{2l(n+1)+(n+2)(n+3)}{2}}\,. \tag{42}$$

where we used the fact that for small frequencies (large distances) $r^2 + a^2 \sim r^2$, $U^t \sim 1$, and $\omega = m\Omega_p \sim m\sqrt{(n+1)M} r_0^{-(3+n)/2}$.

3. Solution X^∞_{kjm}

The solution X^∞_{kjm}, which satisfies outgoing-wave boundary conditions at infinity is quite simple to derive, since for this case the boundary condition is imposed at infinity and we do not need to require regularity at the horizon. The method is analogous to that already described above and can be seen in Ref. [17]. In the low-frequency limit, X^∞_{kjm} is given at leading order and near $z = 0$ by

$$X^\infty_{kjm}(z \ll 1) \sim i^J \frac{2^J}{\sqrt{\pi}}\Gamma[J+1/2] z^{-J}\,. \tag{43}$$

We can now compute the flux across the horizon. Using Eqs. (30) and (31) we get

$$\dot{E}_H = m\Omega_p k_H \left|Z^{r_H}_{kjm}\right|^2 = = m k_H (\alpha\, q_p)^2 \Gamma_1^2 \left(\frac{n+1}{2}\right)^{1/2} r_H (2M)^{\frac{2l+\frac{3n}{2}+\frac{3}{2}}{n+1}} \times |S_{kjm}(\pi/2)|^2 |Y_j(\pi/2,\pi/2,\ldots)|^2 \times r_0^{-\frac{4l+5n+7}{2}}\,, \tag{44}$$

where $\Gamma_1 = \frac{\Gamma[l+n/2+1/2]\Gamma[2-D_*+\alpha-\beta]\Gamma[1+\alpha-\beta]}{2\Gamma[l+n/2+3/2]\Gamma[1+2\alpha]\Gamma[2-D_*-2\beta]}$.

4. Ratio of the fluxes

We can now obtain an expression for the ratio of the fluxes on the horizon and at infinity for general l, m, and

n, as a function of the orbital velocity in $4+n$ dimensions defined by

$$v = [M(n+1)]^{\frac{1}{n+3}}\, \Omega_p^{\frac{n+1}{n+3}} \,. \tag{45}$$

Using the expressions for $\dot{E}_H$ and $\dot{E}_\infty$ calculated above we find

$$\frac{\dot{E}_H}{\dot{E}_\infty} = \frac{k_H r_H \left[2^{l+n/2+1}\Gamma[l+n/2+3/2]\right]^2}{\pi m^{2l+n+1}} \Gamma_1^2 \times \left(\frac{2}{n+1}\right)^{\frac{1+2l+n}{1+n}} \times v^{-\frac{(n-1)(n+1+2l)}{n+1}} \,. \tag{46}$$

For sufficiently small orbital frequencies, such that the superradiance condition is met, and the flux at the horizon is negative, we then find that the ratio between the fluxes *grows* in magnitude with r_0 and the particle is tidally accelerated outward.

Note that these results were derived under the assumption of slow rotation, $a \ll r_H$. This approximation is particularly severe in the near-extremal, five-dimensional case, where $r_H \to 0$. Nevertheless, as we discuss in the next section, our method captures the correct scaling of the energy fluxes for *any* spin, and it even gives overall coefficients that are in very good agreement with the numerical ones in the slowly rotating case. This is shown in Fig. 6, where we compare the analytical results of this section with the numerical fluxes computed in the next section.

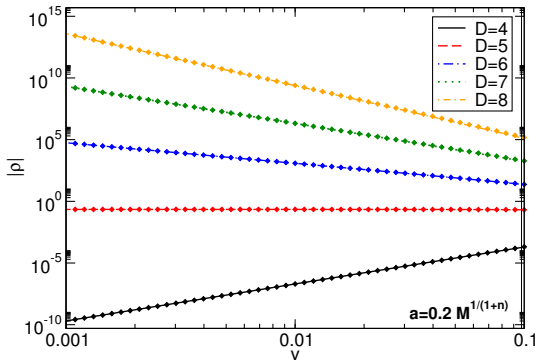

FIG. 6. Comparison between the flux ratio $\rho = \dot{E}_H^{\rm Tot}/\dot{E}_\infty^{\rm Tot}$ (in absolute value) calculated analytically and numerically, as a function of the particle velocity v for $n = 0, 1, 2, 3, 4$ ($D = 4, 5, 6, 7, 8$) and $a = 0.2M^{1/(1+n)}$. The straight curves correspond to the analytical formula with $l = 1$, and the dots are the numerical results discussed in section V B. In the slowly rotating regime, numerical results are in very good agreement with the analytical formula.

B. Numerical Results

The Green function approach described above can be implemented numerically using standard methods Ref. [18, 37, 38]. For given values of r_0, a, and n, we can compute the fluxes by truncating the sum in Eq. (30) to some $k_{\rm max}$, $m_{\rm max}$, and $j_{\rm max}$. As discussed before, for circular orbits only $j = 0$ terms give a nonvanishing contribution.

In Fig. 7 we compare the flux ratio $\rho = \dot{E}_H^{\rm Tot}/\dot{E}_\infty^{\rm Tot}$ as a function of the orbital velocity v for $a = 0.99M^{1/(1+n)}$ in various dimensions. The plots confirm our analytical expectations that the behavior for $n > 1$ ($D > 5$) is qualitatively different: the energy flux across the horizon is larger (in modulus) than the flux at infinity. This figure is analogous to Fig. 6 but for $a = 0.99M^{1/(1+n)}$, i.e. a regime that is not well described by the analytical formula (46). For $D = 4$, we find the usual behavior; i.e. the flux at the horizon is usually negligible with respect to that at infinity, and the ratio decreases rapidly at large distance. The case $D = 5$ marks a transition, because ρ is constant at large distance. This is better shown in the left panel of Fig. 8. On the other hand, for any $D > 5$ the flux across the horizon generically dominates over the flux at infinity.

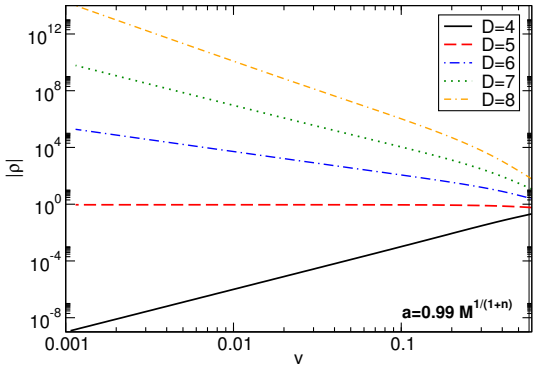

FIG. 7. The flux ratio $\rho = \dot{E}_H^{\rm Tot}/\dot{E}_\infty^{\rm Tot}$ (in absolute value) as a function of the particle velocity v defined in Eq. (45) for $n = 0, 1, 2, 3, 4$ ($D = 4, 5, 6, 7, 8$) and $a = 0.99M^{1/(1+n)}$.

In Fig. 8 we show the flux ratio ρ for some selected value of the spin parameter a in five dimensions (left panel) and in six dimensions (right panel). When $D = 5$, the ratio is constant in the small v region, and it approaches unity in the extremal limit, $a \to \sqrt{2M}$. As shown in the right panel of Fig. 8, when $D = 6$ there exist some orbital velocity for which $-\rho = 1$, corresponding to a total vanishing flux, $\dot{E}_H + \dot{E}_\infty = 0$. These orbital frequencies correspond to "floating" orbits [27, 37]. Although in the right panel of Fig. 8 this is shown only for $a/M^{1/3} = 0.1, 0.2, 0.3$, we expect this to be a generic feature also for larger values of the spin. The poor convergence properties of the series (30) prevent us from extending the curves to larger values of v, where floating orbits for $a > 0.3M^{1/3}$ are expected to occur. At smaller velocity, the energy flux contribution dominates, and the motion of the test particle is generically dominated by tidal acceleration. Similar results can be obtained for any $D \geq 6$.

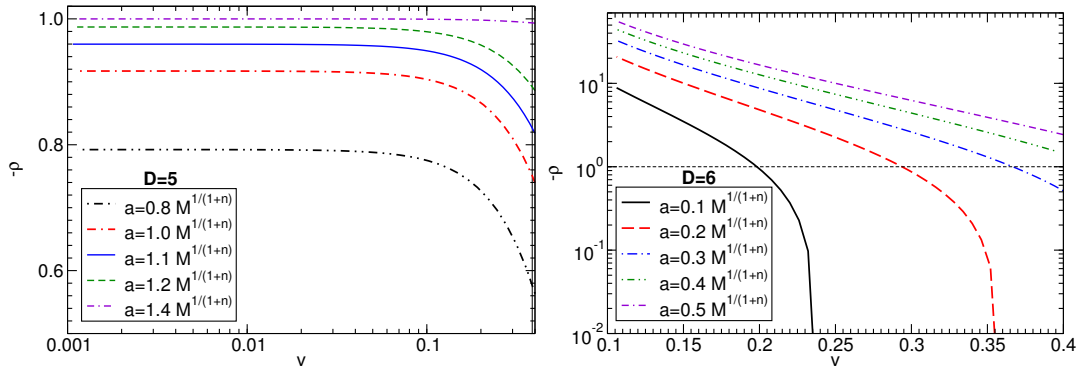

FIG. 8. The ratio $\rho = \dot{E}_H^{\rm Tot}/\dot{E}_\infty^{\rm Tot}$ as a function of the orbital velocity defined in Eq. (45) for several values of a. Left panel: when $D = 5$, the ratio is constant in the small v region, and it approaches unity in the extremal limit, $a \to \sqrt{2M}$. Right panel: when $D = 6$, the flux at the horizon can exceed the flux at infinity. For each curve, the intersection with the horizontal line corresponds to a floating orbit, $-\rho = 1$. Note that, at large orbital velocity, the superradiant condition is not met and $\dot{E}_H > 0$.

VI. CONCLUSIONS

Through the use of black hole perturbation theory, we computed the massive scalar radiation emitted by a test-particle falling radially into a Schwarzschild black hole. The energy spectra suffers a cutoff at the massive scalar field fundamental quasinormal frequency, thus showing the relevance of the quasinormal modes of a black hole. At late times, the lowest multipoles of the massive radiation were shown to be dominated by an oscillatory tail, which decays slower than any power law.

In the second part of this work, we computed the amplification of massless scalar waves scattering off a singly spinning Myers–Perry black hole due to superradiance. In dimensions greater than five, where there is no upper limit on the black hole spin, the amplification factor does not increase without limit when we increase the spin parameter. It was then conjectured that this behavior is due to the asymptotic behaviour of the ergoregion proper volume which, as for the amplification factor, goes to zero for very large spins.

Finally, we concluded with the main result of this paper, by computing the rate at which the energy is extracted from a singly spinning, higher-dimensional black hole when a massless scalar field is coupled to a test particle in circular orbit. We showed that, for dimensions greater than five and small orbital velocities, the energy flux radiated to infinity becomes negligible compared to the energy extracted from the black hole via superradiance. Although we considered scalar-wave emission, we expect our results to be generic in higher dimensions. In particular, superradiance should be a dominant effect also for gravitational radiation. At leading order, the ratio $|\dot{E}_H|/\dot{E}_\infty$ for gravitational radiation should scale with the velocity as described by Eq. (46). The dominant quadrupole term ($l = 2$) reads [28]

$$\frac{|\dot{E}_H|}{\dot{E}_\infty} \sim v^{-\frac{(n-1)(n+5)}{n+1}} .$$

By comparing the formula above to Eq. (46) with $l = 1$, we note that dipolar effects are dominant over their quadrupolar counterpart. Nevertheless, even in the purely gravitational case, tidal acceleration and floating orbits around spinning black holes are generic and distinctive effects of higher dimensions.

In principle, gravitational waveforms would carry a clear signature of floating orbits [37, 38]. Does floating or these strong tidal effects have any significance in higher-dimensional black hole physics? We should start by stressing that circular geodesics in higher dimensions are unstable, on a time scale comparable to the one discussed here [35]; however, our analysis suggests that, while more pronounced for circular orbits, tidal acceleration is generic and in no way dependent on the stability of the orbit under consideration. We are thus led to conjecture that tidal effects are crucial to determine binary evolution in higher dimensions. It is possible that tidal effects already play a role in the numerical simulations of the kind recently reported in Refs. [9, 39, 40], but further study is necessary. One of the consequences of our results for those types of simulations is, for instance, that in higher-dimensional black hole collisions the amount of gravitational radiation accretion might play an important role. It would certainly be an interesting topic for further study to understand tidal effects for generic orbits, and to include finite-size effects in the calculations.

[1] F. Melia, (2007), 0705.1537 [astro-ph].

[2] S. W. Hawking, Commun.Math.Phys. **43**, 199 (1975).

[3] J. M. Maldacena, AIP Conf.Proc. **484**, 51 (1999).
[4] E. Witten, Adv.Theor.Math.Phys. **2**, 253 (1998), hep-th/9802150 [hep-th].
[5] N. Arkani-Hamed, S. Dimopoulos, and G. R. Dvali, Phys.Lett. **B429**, 263 (1998), hep-ph/9803315 [hep-ph].
[6] N. Arkani-Hamed, S. Dimopoulos, and G. R. Dvali, Phys.Rev. **D59**, 086004 (1999), hep-ph/9807344 [hep-ph].
[7] I. Antoniadis, N. Arkani-Hamed, S. Dimopoulos, and G. R. Dvali, Phys.Lett. **B436**, 257 (1998), hep-ph/9804398 [hep-ph].
[8] L. Randall and R. Sundrum, Phys.Rev.Lett. **83**, 4690 (1999), hep-th/9906064 [hep-th].
[9] V. Cardoso, L. Gualtieri, C. Herdeiro, U. Sperhake, *et al.*, (2012), 1201.5118 [hep-th].
[10] S. B. Giddings and S. D. Thomas, Phys.Rev. **D65**, 056010 (2002), hep-ph/0106219 [hep-ph].
[11] S. B. Giddings and E. Katz, J.Math.Phys. **42**, 3082 (2001), hep-th/0009176 [hep-th].
[12] R. C. Myers and M. J. Perry, Annals Phys. **172**, 304 (1986).
[13] D. Ida, Y. Uchida, and Y. Morisawa, Phys.Rev. **D67**, 084019 (2003), gr-qc/0212035 [gr-qc].
[14] V. Cardoso, G. Siopsis, and S. Yoshida, Phys.Rev. **D71**, 024019 (2005), hep-th/0412138 [hep-th].
[15] V. Cardoso and S. Yoshida, JHEP **0507**, 009 (2005), hep-th/0502206 [hep-th].
[16] E. Berti, V. Cardoso, and M. Casals, Phys.Rev. **D73**, 024013 (2006), gr-qc/0511111 [gr-qc].
[17] R. Brito, V. Cardoso, and P. Pani, Phys.Rev. **D86**, 024032 (2012), 1207.0504v2 [gr-qc].
[18] S. L. Detweiler, Astrophys. J. **225**, 687 (1978).
[19] V. Cardoso and J. P. S. Lemos, Phys.Lett. **B538**, 1 (2002), gr-qc/0202019 [gr-qc].
[20] R. A. Konoplya and A. Zhidenko, Rev.Mod.Phys. **83**, 793 (2011), 1102.4014 [gr-qc].
[21] S. Hod and T. Piran, Phys.Rev. **D58**, 044018 (1998), gr-qc/9801059 [gr-qc].
[22] X. He and J. Jing, Nucl.Phys. **B755**, 313 (2006), gr-qc/0611003 [gr-qc].
[23] J. Jing, Phys.Rev. **D72**, 027501 (2005), gr-qc/0408090 [gr-qc].
[24] R. A. Konoplya and C. Molina, Phys.Rev. **D75**, 084004 (2007), gr-qc/0602047 [gr-qc].
[25] Y. B. Zel'dovich, JETP Lett. **14**, 180 (1971).
[26] Y. B. Zel'dovich, Sov. Phys. JETP **35**, 1085 (1972).
[27] W. H. Press and S. A. Teukolsky, Nature **238**, 211 (1972).
[28] V. Cardoso and P. Pani, (2012), 1205.3184 [gr-qc].
[29] P. Pani, E. Barausse, E. Berti, and V. Cardoso, Phys.Rev. **D82**, 044009 (2010), 1006.1863v3.
[30] E. Poisson, Phys.Rev. **D47**, 1497 (1993).
[31] E. Poisson and M. Sasaki, Phys.Rev. **D51**, 5753 (1995), gr-qc/9412027 [gr-qc].
[32] P. Kanti and J. March-Russell, Phys.Rev. **D66**, 024023 (2002), hep-ph/0203223 [hep-ph].
[33] S. Chen, B. Wang, R.-K. Su, and W.-Y. P. Hwang, JHEP **0803**, 019 (2008), 0711.3599 [hep-th].
[34] S. Creek, O. Efthimiou, P. Kanti, and K. Tamvakis, Phys.Lett. **B656**, 102 (2007), 0709.0241v2 [hep-th].
[35] V. Cardoso, A. S. Miranda, E. Berti, H. Witek, and V. T. Zanchin, Phys.Rev. **D79**, 064016 (2009), 0812.1806 [hep-th].
[36] S. A. Teukolsky and W. H. Press, Astrophys.J. **193**, 443 (1974).
[37] V. Cardoso, S. Chakrabarti, P. Pani, E. Berti, and L. Gualtieri, Phys.Rev.Lett. **107**, 241101 (2011), 1109.6021 [gr-qc].
[38] N. Yunes, P. Pani, and V. Cardoso, Phys.Rev. **D85**, 102003 (2012), 1112.3351 [gr-qc].
[39] H. Witek, M. Zilhao, L. Gualtieri, V. Cardoso, C. Herdeiro, *et al.*, Phys.Rev. **D82**, 104014 (2010), 1006.3081 [gr-qc].
[40] H. Okawa, K.-i. Nakao, and M. Shibata, Phys.Rev. **D83**, 121501 (2011), 1105.3331 [gr-qc].